Materials Today: Proceedings xxx (xxxx) xxx

Contents lists available at ScienceDirect

Materials Today: Proceedings

journal homepage: www.elsevier.com/locate/matpr

Experimental evaluation of a novel stability control system for two-wheeled robotic wheelchairs

Mostafa Nikpour [a], Loulin Huang [b,*]

[a] Eight360, Research and Development Sector, Wellington 5012, New Zealand
[b] School of Engineering, Computer and Mathematical Sciences, Auckland University of Technology, Auckland 1010, New Zealand

ARTICLE INFO

Article history:
Available online xxxx

Keywords:
Two-wheeled robotic wheelchair
Stability control
Energy consumption

ABSTRACT

A conventional robotic wheelchair containing four wheels (two active driving wheels and two passive casters) is statically stable with poor manoeuvrability. In comparison, a two-wheeled robotic wheelchair (TWRW) without the support of casters offers much better manoeuvrability but is inherently unstable and requires a stability control. Most stability controllers rely on the driving torques of the wheels which are high in magnitude and result in large energy consumption. Various disturbances in the system also affect the performance of the controller.

To address these problems, this paper presents a novel control approach where the stability control is achieved through the motion of a pendulum-like movable mechanism added to the TWRW. A scaled-down TWRW is designed to evaluate the performances of the controllers based on PID control and second order sliding mode control (SOSMC). Experimental results show that under the proposed controller approach, the stability of the TWRW is achieved with much less torque, power, and energy consumption than the conventional control systems.

1. Introduction

Wheelchairs are essential to provide mobility for the elderly or handicapped people [1]. Robotic wheelchairs have become popular as they are easy to use and move without consuming the energy of the riders [2]. A typical robotic wheelchair is four-wheeled (two driving wheels and two casters) which is statically stable but has a poor maneuverability for it cannot make a spot turn or maneuver in a narrow space, and cannot move easily on uneven surfaces [3]. To resolve these problems, two-wheeled robotic wheelchair (TWRW) with a better maneuverability is proposed [45]. Contrary to conventional robotic wheelchairs which have two casters, the TWRW has no caster and is equipped with only two driving wheels [6]. Without the support of casters, it becomes inherently unstable and an active controller is needed to keep it stable [7].

The stability of TWRW is measured by how well it can be kept at the upright position [8]. Most conventional stability control systems rely on the torques applied to the driving wheels [9]. In this control system, the wheels are responsible for the motion and stability of the TWRW at the same time. When a TWRW moves with high acceleration, it is likely the torque and power delivered from the motors are huge [10]. Motors with high power and torque capacity are usually costly and bulky, and high energy consumption reduces the battery's working time before being recharged. Stability control systems based on the movable seat or a movable mass under the rider's seat are developed to solve this problem, but they are limited by the working space for linear motions they require [11]. Stability controllers can be model-free (e.g., PID control, Fuzzy control, etc.) or model-based (e.g., second-order Sliding mode control (SOSMC), computed torque control, etc.). Model-based controllers developed from the dynamic model of the system are more robust than model-free controllers [12]. SOSMC is one of the most common model-based controllers used for its computational efficiency and the robustness of the controlled system it can achieve [13].

In this paper, a novel stability control system where a pendulum-like movable mechanism is added to the TWRW is proposed. Through the motion control of this mechanism, the centre of gravity of the TWRW system including the rider can be varied to keep its stability. The controllers based on PID and SOSMC are implemented. A scaled-down TWRW is designed to validate the

* Corresponding author.
E-mail address: loulin.huang@aut.ac.nz (L. Huang).

https://doi.org/10.1016/j.matpr.2023.04.691
2214-7853/

Please cite this article as: M. Nikpour and L. Huang, Experimental evaluation of a novel stability control system for two-wheeled robotic wheelchairs, Materials Today: Proceedings, https://doi.org/10.1016/j.matpr.2023.04.691

effectiveness of the control system. The rest of the paper is organised as follows.

In Section 2, the structure of a TWRW with the proposed added mechanism is described. The TWRW prototype built for experimental test are explained in Section 3. In Section 4, the experimental results are represented and discussed, and finally conclusions are presented in Section 5.

2. System and controllers description

A TWRW consists of two wheels and a seat for the rider which can rotate freely around the wheels' axle. The seat and the rider are combined to form a body. In the proposed system, a pendulum-like movable mechanism is placed under the seat to assist the wheels for stability and direction control. This mechanism consists of a rod and a mass placed at one end of the rod. The mass of the rod is small and is neglected. Fig. 1a and b show the schematic view of the TWRW and the proposed mechanism from the side and top views, respectively. The mass of each wheel, body, and movable mechanism are denoted by m_w, m_b, and m_p, respectively. The radius of each wheel and the length of the wheels' axle are denoted by r, and d, respectively. The middle of the wheels' axle is shown by O, and P is the point that movable mechanism is added to the system. l is the distance between the body's centre of gravity (COG), and point O, and the length of the movable mechanism's rod is denoted by l'. The distance between point O and P is denoted by b.

To define parameters, two coordinate systems are defined. $X^W - Y^W - Z^W$ is the world coordinate frame which is fixed to the ground. $X^L - Y^L - Z^L$ is the coordinate frame attached to the middle of the wheels' axle. The rotation angles of the right and left wheels measured from the Y^L axis are denoted by θ_r and θ_l, respectively. The rotation angle of the body (pitch angle) is measured from the Y^L axis and shown by θ_b. θ_p denotes the rotation angle of the movable mechanism measured from link OP. The moment of inertia of each wheel is denoted by J_{w_x}, J_{w_y}, and J_{w_z}. Also, the moment of inertia of the body is denoted by J_{b_x}, J_{b_y}, and J_{b_z}. J_{p_x}, J_{p_y}, and J_{p_z} denote the moment of inertia of the movable mechanism. τ_r, τ_l, and τ_p denote the input torque of the right wheel, left wheel, and movable mechanism, respectively. Their input powers are denoted by P_r, P_l, and P_p, respectively. E_r, E_l, and E_p are used to denote their energy consumption, respectively.

The dynamic model of the system is described by

$$M_p\ddot{q}_p + C_p\dot{q}_p + G_p = B_p\tau_p$$

$$q_p = \lfloor\theta_r\theta_l\theta_b\theta_p\rfloor^T,\ \tau_p = \lfloor\tau_r\tau_l\tau_p\rfloor^T$$

$$B_p = \begin{bmatrix}1000\\0100\\0001\end{bmatrix},\ G_p = \begin{bmatrix}0\\0\\-(M_bl + M_pb)g\sin\theta_b + M_pgl'\sin(\theta_b+\theta_p)\\M_pgl'\sin(\theta_b+\theta_p)\end{bmatrix}$$

and the other 4 times 4 matrices in the equation are defined by the system parameters and states.

The following are the expressions of the stability controllers.

- PID controller

$$\tau_p = K_d\dot{\theta}_b + K_p\theta_b + K_i\int_0^t \theta_b dt$$

- SOSMC controller

$$\tau_p = \frac{-A_{p3} - c\dot{\theta}_b - \lambda|\sigma|^{0.5}\text{sign}(|\sigma|) + v}{\widehat{M}_{p34}^{-1}}$$

$$\sigma = \theta_b + c\dot{\theta}_b$$

$$\begin{aligned}A_{p3} = & -\widehat{M}_{p31}^{-1}\left(C_{p11}\dot{\theta}_r + C_{p12}\dot{\theta}_l + C_{p13}\dot{\theta}_b + C_{p14}\dot{\theta}_p\right)\\ & -\widehat{M}_{p32}^{-1}\left(C_{p21}\dot{\theta}_r + C_{p22}\dot{\theta}_l + C_{p23}\dot{\theta}_b + C_{p24}\dot{\theta}_p\right)\\ & -\widehat{M}_{p33}^{-1}\left(C_{p31}\dot{\theta}_r + C_{p32}\dot{\theta}_l + C_{p33}\dot{\theta}_b + C_{p34}\dot{\theta}_p + G_{p3}\right)\\ & -\widehat{M}_{p34}^{-1}\left(C_{p41}\dot{\theta}_r + C_{p42}\dot{\theta}_l + C_{p43}\dot{\theta}_b + G_{p4}\right)\end{aligned}$$

$$M_{p34} = M_pl'^2 - M_pbl'\cos\theta_p + J_{p_z}$$

$$\dot{v} = \begin{cases}-u, |u| > U_M\\ -\alpha\text{sign}(\sigma), |u| \le U_M\end{cases}$$

$$u = -\lambda|\sigma|^{0.5}\text{sign}(|\sigma|)$$

All the constants in the controllers are control parameters.

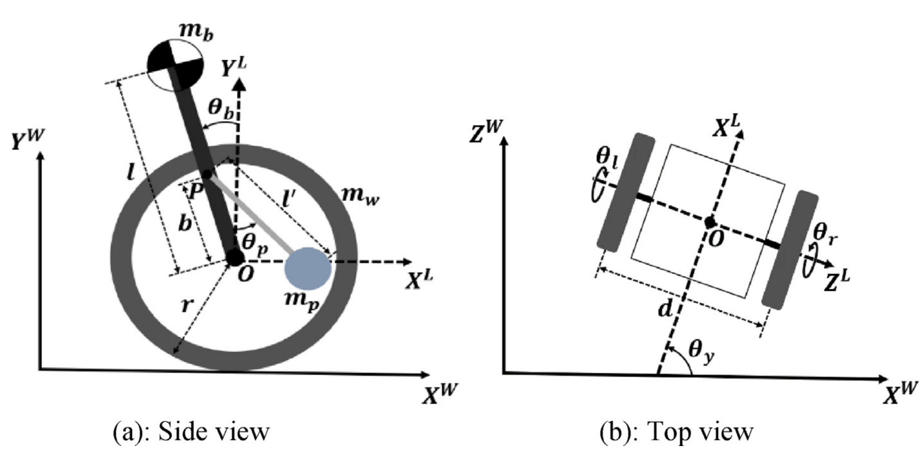

Fig. 1. Schematic view of the TWRW and the proposed mechanism.

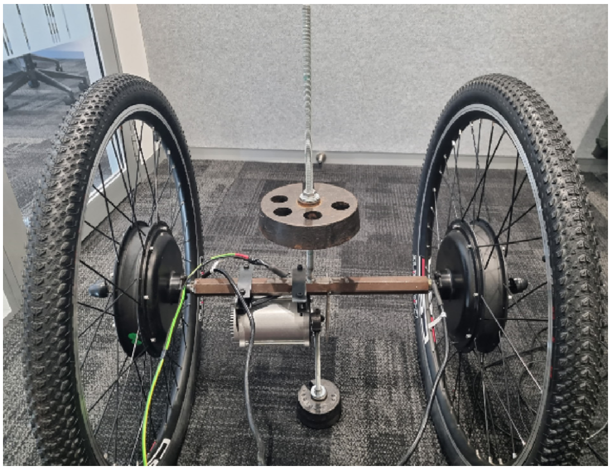

Fig. 2. The scaled-down model of the TWRW.

3. Experimental setup

The TWRW prototype designed in this paper consists of two driving wheels equipped with brushless direct current (BLDC) motors. The wheels are connected to each other through a steel axle. The axle is lubricated well, which allows the wheels to freely rotate around the axle. Additionally, there is no clearance between the wheels' shafts and the axle. A light steel rod which its mass can be neglected is welded from one end to the middle of the wheels' axle. The 5 kg steel mass is connected to the rod and placed at the top of the wheels' axle. This mass can be considered as the body (seat and rider) in a full-scaled TWRW. A pendulum-like movable mechanism which comprises a light rod and a 2 kg steel mass placed at one end of the rod is placed under the wheels' axle and is able to freely rotate by a direct current (DC) motor around the motor's shaft. The input current and voltage of all motors are supplied by a 14 cell lithium battery. Fig. 2 shows the real model of TWRW prototype and its system parameters are listed in Table 1.

The controller's feedback are obtained using two IMU sensors including VN-200 and MPU6050. The VN-200 and MPU6050 are attached to the body and the movable mechanism, respectively to measure their angles and velocities. According to the feedback values, the input torque of the right and left wheels for the conventional system and the input torque of the movable mechanism for the proposed system are computed. The MyRIO-1900 microcontroller is used to calculate the input torque and send the data to the Arduino mega 2560 by the universal asynchronous receiver/-transmitter (UART) signals. The motor controller is a bridge between the microcontrollers and motors. The MTVESC50A which is a programmable motor controller is used for the experimental setup. Through MTVESC50A, the current, speed, etc. of motors can be controlled.

Table 1
System parameters of the TWRW prototype.

Property	m_w	m_b	m_p	$J_{w_x}, J_{w_y}, J_{w_z}$	$J_{b_x}, J_{b_y}, J_{b_z}$	$J_{p_x}, J_{p_y}, J_{p_z}$	r	d	b	l	l'
Value	10	5	2	0.32, 0.32, 0.64	0.02, 0.01, 0.01	0.002, 0.001, 0.001	0.37	0.5	0	0.15	0.25
Unit	kg	kg	kg	Kg.m^2	Kg.m^2	Kg.m^2	m	m	m	m	m

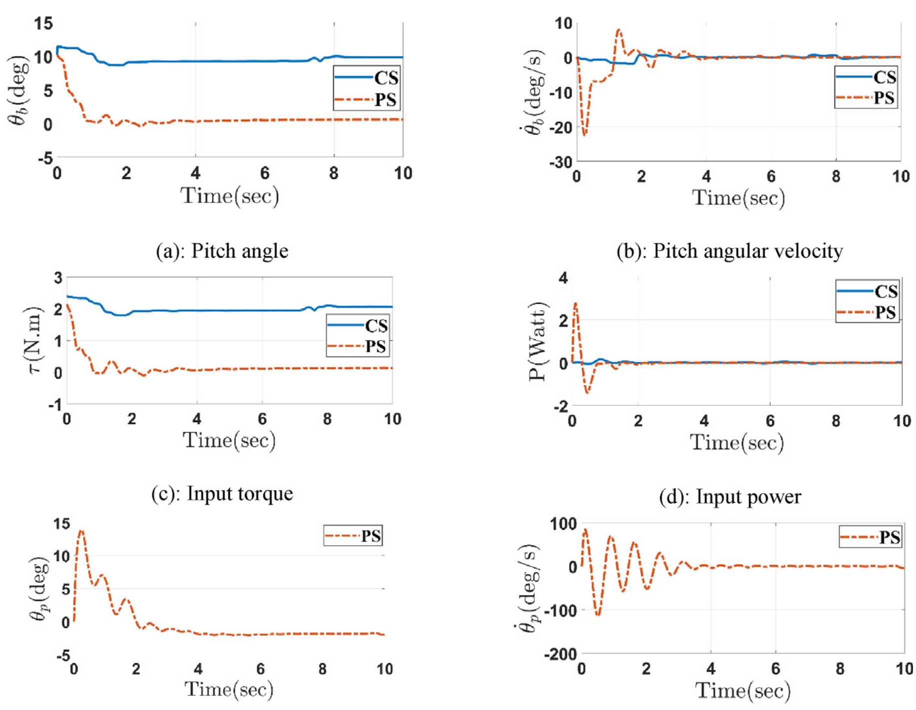

(a): Pitch angle (b): Pitch angular velocity
(c): Input torque (d): Input power
(e): Movable mechanism angle (f): Movable mechanism angular velocity

Fig. 3. The TWRW experimental results for the stability control of the conventional system (CS) and the proposed system (PS) through PID control.

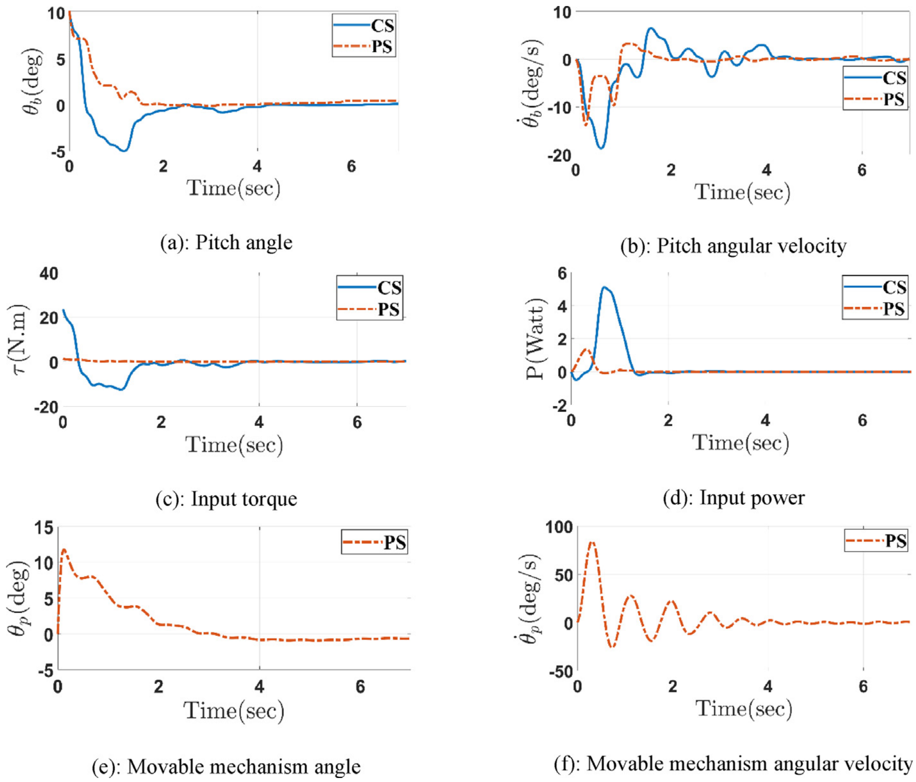

Fig. 4. The TWRW experimental results for the stability control of the conventional system (CS) and the proposed system (PS) through SOSMC.

Table 2
Energy consumption of the conventional and the proposed systems.

Energy Consumption	Conventional Method -PID	Proposed Method -PID	Conventional Method -SOSMC	Proposed Method -SOSMC
Value	0.2108 J	0.9610 J	2.8138 J	0.4750 J

4. Results

To analyse the performance of the stability control, the TWRW prototype is tested with non-zero initial pitch angle. The initial pitch angle is set to 10*deg*. The controller gains of PID and SOSMC chosen for conventional and proposed system are same. Fig. 3 represents the experimental results of stability control for the conventional and proposed systems through PID control. It can be seen that the pitch angle converges to zero in the proposed system, while it remains almost unchanged in the conventional system (see Fig. 3a). Fig. 3b depicts the pitch angular velocity which converges to zero under both control systems. The required input torque for stability can be seen in Fig. 3c, where both control methods require almost same initial torque. The input torque almost stays on its initial value in the conventional system, while it converges to zero in the proposed approach. It can be concluded that the initial torque in the conventional system is not enough to move the left and right wheels. However, it is enough for the movable mechanism to stabilize the wheelchair. The input power in both control methods are shown in Fig. 3d, where it doesn't change and remains zero in the conventional system as the driving wheels don't move. Whereas, the oscillation of input power can be seen in the proposed system which converges to zero when the TWRW reaches its stability. The angle and angular velocity of movable mechanism in the proposed method are depicted in Fig. 3e and f, respectively. They show that the range of angular motion and velocity of the movable mechanism are small and in an acceptable range which doesn't affect the rider's comfort.

The experimental results of the TWRW stability control under both control systems through SOSMC are represented in Fig. 4. It can be seen that the pitch angle and pitch angular velocity under both control approaches converge to zero, while they have less oscillation and faster convergence to zero in the proposed system than conventional one (see Fig. 4a, b). In addition, the required input torque and power in the proposed system are much lower than the conventional approach (see Fig. 4c, d). The angle and angular velocity of the movable mechanism depicted in Fig. 4e, f, respectively show that they are very small and the movable mechanism can be operated with no effect on the comfort of rider. The energy consumption under both control systems through PID and SOSMC are listed in Table. 2. It can be seen that the energy consumption of the motors for the conventional system in PID are almost zero as the input power of the driving wheels are near zero. The input torque and power are small and insufficient to drive the wheels, which causes failing control systems. While, the energy consumption in SOSMC for the proposed method are significantly lower than those obtained in conventional approach, where both methods could stabilize the system.

5. Conclusion

In this paper, a novel approach is proposed for the stability control of TWRW. A pendulum-like movable mechanism is added to the wheelchair to keep it stable. In this system, the torque is applied to the added mechanism, while in the conventional system the torque is applied to the right and left wheels. The PID and

SOSMC control schemes are used for stability control. The scaled-down prototype is built to achieve the experimental results. The prototype is equipped with two BLDC driving wheels and a DC motor to power the movable mechanism. The high-accuracy IMU sensor (VN-200) is used to measure the pitch angle and its velocity, and a MPU6050 sensor is attached to the added mechanism to measure its angle and angular velocity. The experimental results demonstrate that in the proposed approach, the stability of TWRW is achieved, while the input torque, input power, and energy consumption for the control system are much lower than the conventional method.

Data availability

The data that has been used is confidential.

Declaration of Competing Interest

The authors declare that they have no known competing financial interests or personal relationships that could have appeared to influence the work reported in this paper.

References

[1] H.A. Yanco, Wheelesley: a robotic wheelchair system: Indoor navigation and user interface, in: Assistive Technology and Artificial Intelligence, Springer, 1998, pp. 256–268.

[2] L. Fehr, W.E. Langbein, S.B. Skaar, Adequacy of power wheelchair control interfaces for persons with severe disabilities: a clinical survey, J. Rehabil. Res. Dev. 37 (3) (2000) 353–360.

[3] C. Bühler, R. Hoelper, H. Hoyer, W. Humann, Autonomous robot technology for advanced wheelchair and robotic aids for people with disabilities, Rob. Auton. Syst. 14 (2–3) (1995) 213–222.

[4] S. Ahmad, M.O. Tokhi, N. Siddique, Modular fuzzy control with input shaping technique for transformation of two-wheeled wheelchair to four-wheeled mode, in: 2010 IEEE Symposium on Industrial Electronics and Applications (ISIEA), IEEE, 2010, pp. 562–566.

[5] A. Dinale, K. Hirata, T. Murakami, Analytical design of a robust motion controller for a two-wheeled wheelchair system, in: 2013 16th International Conference on Advanced Robotics (ICAR), IEEE, 2013, pp. 1–6.

[6] N. Abdul Ghani, M.O. Tokhi, Sit-to-stand and stand-to-sit control mechanisms of two-wheeled wheelchair, J. Biomech. Eng. 138 (4) (2016).

[7] N. Hirata, T. Murakami, An approach to safety mechanism and control for improved operability in two-wheeled wheelchair, in: 2014 10th France-Japan/ 8th Europe-Asia Congress on Mecatronics (MECATRONICS2014-Tokyo), IEEE, 2014, pp. 121–126.

[8] D. Xia, Y. Yao, L. Cheng, Indoor autonomous control of a two-wheeled inverted pendulum vehicle using ultra wide band technology, Sensors 17 (6) (2017) 1401.

[9] N. Minouchehr, S.K. Hosseini-Sani, Design of model predictive control of two-wheeled inverted pendulum robot, in: 2015 3rd RSI International Conference on Robotics and Mechatronics (ICROM), IEEE, 2015, pp. 456–462.

[10] M. Nikpour, L. Huang, A.M. Al-Jumaily, Stability and direction control of a two-wheeled robotic wheelchair through a movable mechanism, IEEE Access 8 (2020) 45221–45230.

[11] Y. Sago, Y. Noda, K. Kakihara, K. Terashima, Parallel two-wheel vehicle with underslung vehicle body, Mech. Eng. J. 1 (4) (2014) DR0036–DR0036.

[12] S. Nithya, N. Sivakumaran, T. Balasubramanian, N. Anantharaman, Model based controller design for a spherical tank process in real time, IJSSST 9 (4) (2008) 25–31.

[13] E.-H. Zheng, J.-J. Xiong, J.-L. Luo, Second order sliding mode control for a quadrotor uav, ISA Trans. 53 (4) (2014) 1350–1356.